Korean J. Chem. Eng., 17(3), 273-279 (2000)

The Characteristics of Particle Flow in the Overflow and Underflow Standpipe of Fluidized Beds

Ji-Min Kim, Gui Young Han† and Chang Keun Yi*

Department of Chemical Engineering, Sungkyunkwan University, Suwon, Korea
*Korea Institute of Energy Research, Taejon, Korea
(*Received 30 September 1999 • accepted 2 February 2000*)

Abstract–Characteristics of particle flow in the standpipes of a 10 cm I.D.×120 cm high fluidized bed were investigated. The standpipes used in this experiment were vertical overflow and vertical underflow standpipes. Sand particles and polyethylene powders were employed as the bed materials. The effects of standpipe diameter, gas velocity and particle properties on the solid flow rate were determined. The experimental results showed that the flow behaviors of solids through the overflow and underflow standpipes are different with variations of operating conditions. For both standpipes, the mass flow rate of solids was strongly dependent on the standpipe diameter. For the overflow standpipe, the increase of gas velocity increased the solids flow rate. But for the underflow standpipe it decreased the solid flow rate. From the measured pressure drops, solid fractions in the standpipes were determined by the momentum balance. The obtained experimental data of solids mass flow rate were well correlated with the pertinent dimensionless groups for underflow as well as overflow standpipes.

Key words: Standpipe, Fluidized Bed, Solid Mass Flow Rate, Void Fraction

INTRODUCTION

Standpipes are used to convey particulate solids from a region at lower pressure to higher pressure with the help of gravity, and these devices are considered to be a vital link to the circulating fluidized bed system [Ginestra et al., 1980]. A circulating fluidized bed consists of a riser, cyclones and standpipe. The standpipes transfer solids from a point of lower pressure to a point of higher pressure, provide a seal against undesirable gas flow in one direction, and regulate solids circulation. A standpipe can achieve these three capabilities only within a restricted range of operating conditions. Failure to do so would lead to interruption of solid flow and plant shutdown [Rudolph et al., 1991; Zhang, 1998]. Processes incorporating standpipes are often disrupted by sudden unexpected instabilities in their operation. Although standpipes have been used for many years, their design is entirely based on 'rules of thumb' and actual operation experiences [Leung, 1977; Jones, 1978], and the mechanism of their operation is poorly understood. This is particularly unfortunate since standpipes are well known for developing instability in certain circumstances, causing a transition to a state with inadequate pressure build-up in the pipe [Ginestra et al., 1980]. Two types of standpipes are widely used in fluidized bed processes: the overflow standpipe and the underflow standpipe. The pressure drop in a standpipe is balanced automatically and these characteristics are different between overflow and underflow standpipe [Grace et al., 1996; Rhodes, 1998].

†To whom correspondence should be addressed.
E-mail: gyhan@skku.ac.kr
This paper was presented at the 8th APCChE (Asia Pacific Confederation of Chemical Engineering) Congress held at Seoul between August 16 and 19, 1999.

The objective of this study is to examine the effect of standpipe diameter, gas velocity and properties of employed particles on the flow rate of solids from the upper fluidized bed to a lower fluidized bed and to propose a correlation of solid flow rate as a function of relevant operating variables for each type of standpipe. Solid fraction in the standpipe is also determined from the measurement of pressure drop in the pipe.

EXPERIMENTAL

The experimental test facility used in this study is shown in Fig. 1. The test section consisted of upper and lower fluidized beds and a standpipe was located between the fluidized beds. The fluidized bed was made of acrylic column with inside diameter of 10 cm and height of 60 cm each. The gas distributor was porous plate and four pressure taps were mounted at the bottom, top and between the distributors of the test section as shown in Fig. 1. Pressure taps were connected to the pressure transducers and the measured pressure drop data were stored in a PC through the data acquisition unit every 2 seconds. The distributor located between the upper and lower fluidized bed was designed to accommodate the different dimensions of standpipes. The fluidizing gas was provided from a blower to the bottom of the lower bed and the gas leaving the lower bed was bypassed to the distributor of the upper bed. Two different dimensions of overflow and underflow standpipes were employed. The diameters of the underflow standpipe (d_{sp}) were 1.14 cm, and 2.53 cm, respectively, and the length was 10 cm. The diameters of the overflow standpipe were 1.14 cm, and 2.53 cm and the length below the distributor of the upper bed was 40 cm so that the standpipe outlet was immersed into the static height of the lower bed and the height of standpipe inlet was 5 cm above the distributor of the upper bed. Fig. 1(a) shows the experimental set-up of the overflow stand-

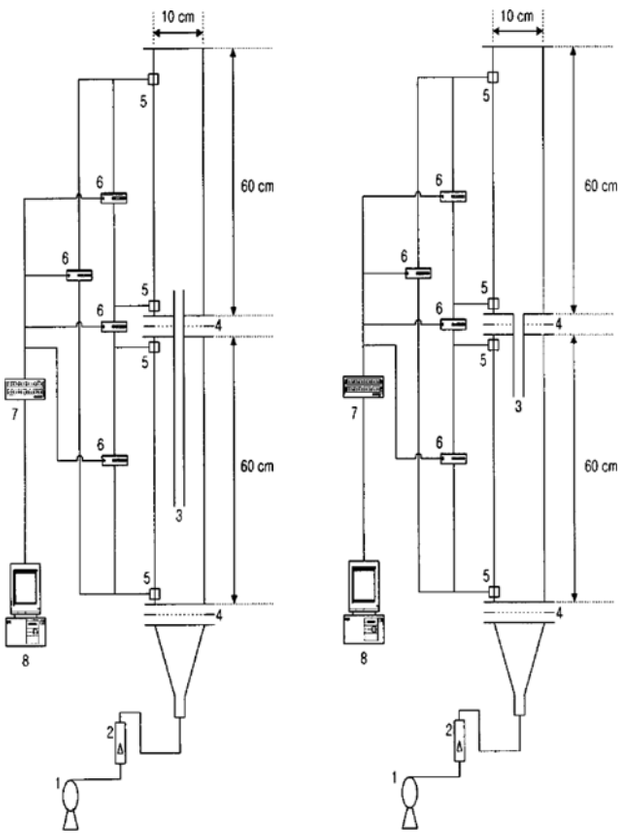

Fig. 1. Schematic diagram of standpipe experimental test set-up.

Table 1. Physical properties of employed particles

Properties\Particle	Sand	Sand	PE
Mean diameter (μm)	280	147	366
Bulk density (kg/m^3)	1850	1877	400
Particle density (kg/m^3)	2650	2780	800
Minimum fluidized velocity (cm/sec)	7.20	2.08	2.54

pipe system and Fig. 1(b) shows the experimental set-up of the underflow standpipe system. The experimental data were obtained at atmospheric pressure and room temperature. The experimental procedure was as follows. The inlet of the standpipe was blocked by rubber cock, the bed material was charged about 50% by bed volume, and air was introduced to the lower fluidized bed. When the upper fluidized bed reached steady state, the rubber cock was removed and the particles began to flow down to the lower bed through the standpipe. The solid mass flow rate transported through the standpipe was determined by measuring the increase of static head of the lower bed or decrease of static head of the upper bed. The calibration curve for pressure drop and solid mass flow rate was prepared from the preliminary test of the measured pressure drop and the weight of the solid particles. The bed materials were 147 micron, 280 micron sand particles and the 366 micron polyethylene powders. The physical properties of the employed particles are shown in Table 1.

RESULTS AND DISCUSSION

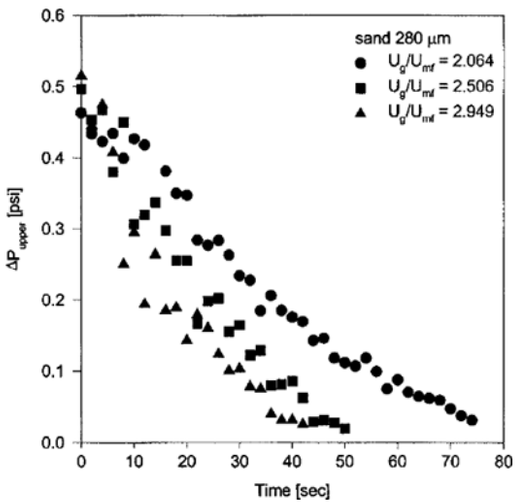

Fig. 2. The solid flow rate as a function of time in the overflow standpipe.

1. Overflow Standpipe

Little research work has been carried out on the characteristics of overflow standpipes. In general, the exit of the overflow standpipe is immersed in the lower bed of particles; the solids in the overflow standpipe are transported as the packed bed mode [Geldart, 1986]. Even in the underflow standpipe configuration, with the control of valve opening the solid flow in the standpipe is transported as a packed bed mode [Leung, 1997, 1978; Zhang et al., 1998]. From visual observation, it was found that the flow regime of gas-solid suspension flow in the standpipe was packed bed mode.

The time series of pressure drop for the standpipe diameter of 2.53 cm with sand particle at different gas velocities is shown in Fig. 2. As shown in Fig. 2, the slope of pressure drop, which is corresponding to the solid mass flow rate from the upper to the lower bed, is almost linear at three different gas velocities. This means that the solid mass flow rate is independent of the static bed height.

The effect of gas velocity on the solid mass flow rate is shown in Fig. 3 for three different types of particles and two different diameters of standpipe. As can be seen in Fig. 3, at the lower gas velocity region (U_g/U_{mf}<3.0), the increase of gas velocity increased the solid mass flow rate. This may be due to the fact that at the lower gas velocity condition, the increase of gas velocity increased the fluidization quality so the fluidization regime of the upper bed became smooth, bubbling fluidization. But at the higher gas velocity region (U_g/U_{mf}>3.0), the increase of gas velocity increase the upward gas velocity in the standpipe and the flow regime of upper bed became slugging fluidization; thus the downward flow of solid decreased. From Fig. 3, it was also found that for the sand particles the effect of particle size was insignificant and the diameter of the standpipe affected the solid flow rate significantly.

2. Underflow Standpipe

Geldart [1986] suggested that for the operation of an underflow standpipe, it is desirable to install the valve at the end of the standpipe to control the mass flow rate of particles and pres-

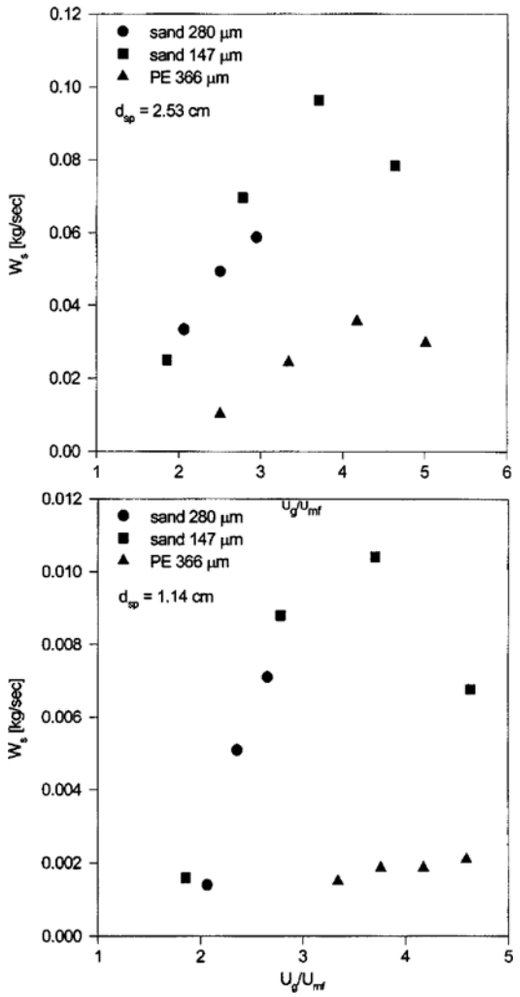

Fig. 3. The effect of gas velocity on the solid flow rate in the overflow standpipe.

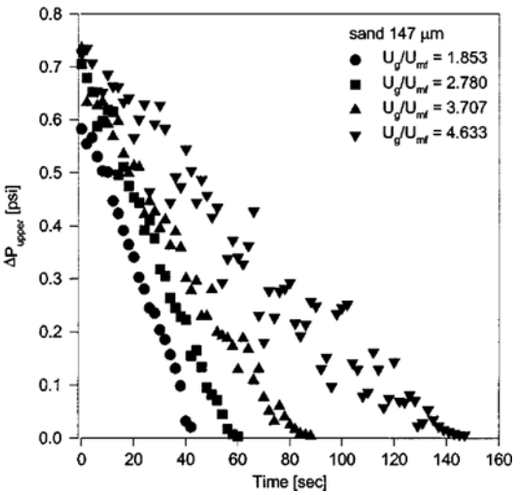

Fig. 4. The solid flow rate as a function of time in the underflow standpipe.

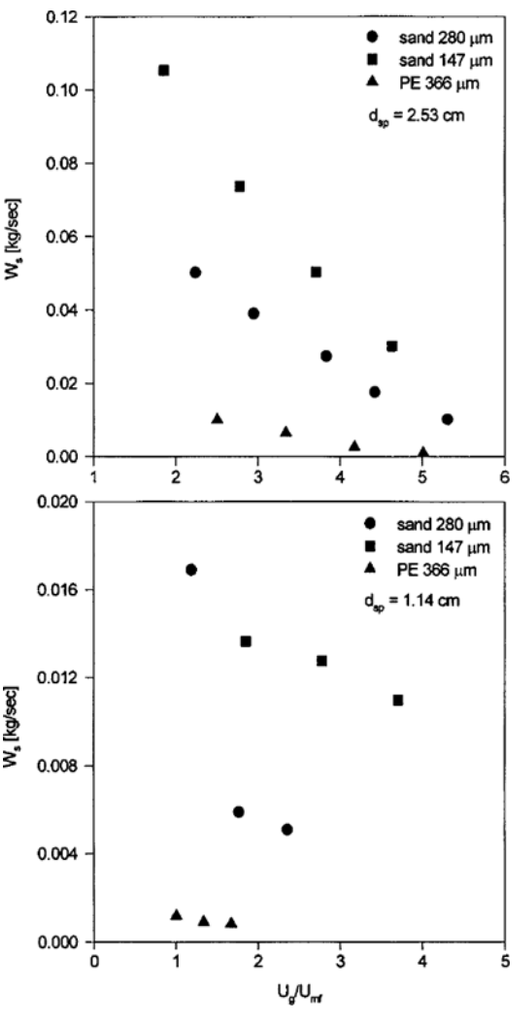

Fig. 5. The effect of gas velocity on the solid flow rate in the underflow standpipe.

sure balance in the loop. Some research work was carried out on the characteristics of an underflow standpipe with a valve at the exit of the standpipes [Jones et al., 1978; Leung, 1977, Knowlton et al., 1978; Ozawa et al., 1991; Picciotti, 1995]. In contrast to the above experimental configurations, in this study the characteristics of an underflow standpipe without valves was investigated to maintain the fluidized bed flow of solids in the standpipe. The significant difference of flow regime of the gas-solid suspension flow in the underflow standpipe without valve was observed. From visual observation, it was found that the flow of suspension in the standpipe was lean-phase flow due to larger amounts of gas flowing into the standpipe exit where there is no flow restriction devices such as valve or orifice.

The time series of the pressure drop for the standpipe diameter of 2.53 cm with sand particles at different gas velocity is shown in Fig. 4. As in the case of overflow standpipe, the slope of the pressure drop is almost linear for the different gas velocity. Therefore, the bed height is not an important operating condition for underflow standpipe operation.

The effect of gas velocity on the solid mass flow rate is shown in Fig. 5. Unlike the overflow standpipe, the increase of gas velocity decrease of the solid flow rate for three different types of employed particles. Zhang et al. [1998] also reported that the

solid mass flow rate in the standpipe was decreased with increased gas velocity. This may be due to the fact that the leg of the overflow standpipe was immersed in the lower section of the packed or fluidized bed so that gas flow rate from the lower bed to the standpipe was smaller than that of the underflow standpipe. Since gas flow rate to the underflow standpipe was larger, drag force acting on the downward particles became greater; thus the flow rate of downward solids significantly decreased in spite of smooth fluidization in the upper fluidized bed. It was also found that unlike the overflow configuration, in the underflow standpipe the effect of particle size on the solid mass flow rate was significant. It may be guessed that drag force acting on the particle is proportional to particle diameter; thus the net downward velocity of solid particle decreased with increasing particle size at the same operating conditions.

3. Proposed Correlation for Standpipes

Based on the experimental data, the following correlations for solid mass flow rate in the overflow and underflow standpipe were obtained.

a) correlation for solid mass flow in the overflow standpipe

$$W_s[\mathrm{kg/hr}]=0.9155(U_g/U_{mf})^{1.7308}(d_{sp}[\mathrm{cm}])^{2.8548}(\rho_s[\mathrm{g/cm^3}])^{1.0213}$$

for $U_g/U_{mf}<4.5$

b) correlation for solid mass flow in the underflow standpipe

$$W_s[\mathrm{kg/hr}]=10.2778(U_g/U_{mf})^{-0.8925}(d_{sp}[\mathrm{cm}])^{2.4385}(\rho_s[\mathrm{g/cm^3}])^{1.6632}(N_{Re,p})^{-0.3192}$$

The comparisons of the proposed correlation with the experimental data for overflow and underflow are shown in Fig. 6 and Fig. 7, respectively. As expected, the solid flow rate was strongly dependent on the standpipe diameter, gas velocity and particle density. The effect of particle size was insignificant for the overflow standpipe.

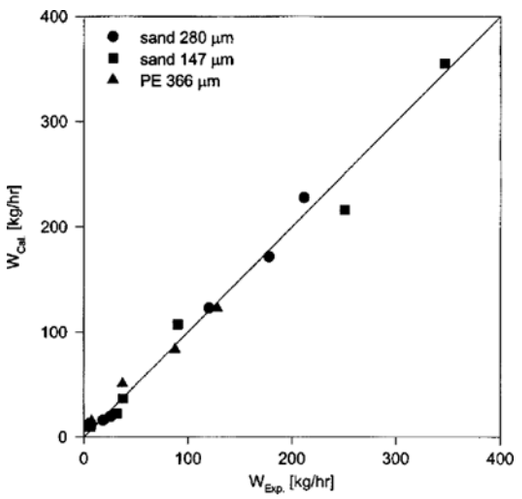

Fig. 6. Comparison of experimental data with calculated values in the overflow standpipe.

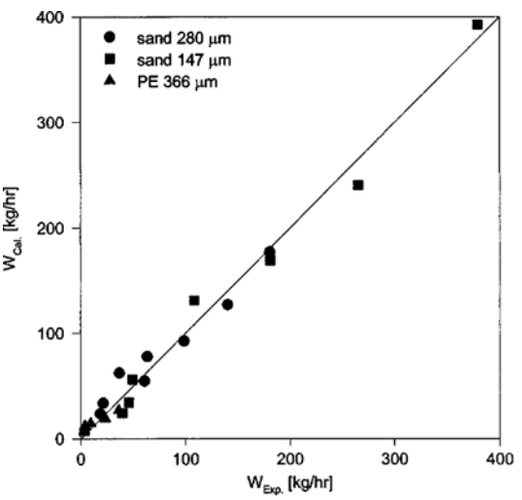

Fig. 7. Comparison of experimental data with calculated values in the underflow standpipe.

4. Estimation of Void Fraction and Solid Velocity in Standpipes

The solid fraction in the standpipe is essential information to understanding the solid flow behavior in the standpipe. Hinze proposed a solid mixture momentum equation for the prediction of solid fraction and pressure drop in the flow of gas-solid mixture as shown in Eq. (1) [Davidson et al., 1985].

$$\frac{d\sigma_z}{dz}+\frac{dP_{sp}}{dz}+\frac{4\tau_w}{d_{sp}}-\rho_s(1-\varepsilon)g+U_s(1-\varepsilon)\rho_s\frac{dU_s}{dz}=0 \tag{1}$$

In case of the overflow standpipe, because its exit is immersed in the lower fluidized bed, the flow pattern of solids is transition packed bed flow or packed bed flow. Therefore, the vertical normal stress in the solid cannot be ignored. For a Coulombic solid the wall shear stress τ_w can be estimated by

$$\tau_w=f\sigma_r \tag{2}$$

$$\sigma_r=\sigma_z\frac{(1+\sin\delta)}{(1-\sin\delta)} \tag{3}$$

The coefficient of friction between solid and wall surface was determined as follows [Leva, 1959].

$$f=\frac{100}{N_{Re,p}} \tag{4}$$

Where, $N_{Re,p}=d_pG_g/\mu_g$ ($N_{Re,p}<20$). σ_z was calculated with the proposed equation of Ginestra et al. [1980] as shown in Eq. (5).

$$\sigma_z=\frac{W^2}{2\rho_s(1-\varepsilon_{mf})}\left(\frac{1}{1-\varepsilon}-\frac{1}{1-\varepsilon_{mf}}\right) \tag{5}$$

By assuming that the vertical normal stress in the solid is constant in the z direction and applying Eqs. (2), (3), (5) into Eq. (1) to lead to Eq. (6).

$$\Delta P_{sp}+\frac{2fW^2}{d_{sp}\rho_s(1-\varepsilon_{mf})}\left(\frac{1}{1-\varepsilon}-\frac{1}{1-\varepsilon_{mf}}\right)\frac{(1+\sin\delta)}{(1-\sin\delta)}z+\frac{W^2}{2\rho_s(1-\varepsilon_{mf})}\left(\frac{1}{1-\varepsilon}-\frac{1}{1-\varepsilon_{mf}}\right)-\rho_s(1-\varepsilon)gz+\frac{W^2}{\rho_s(1-\varepsilon)}=0 \tag{6}$$

Where, $\delta=60^\circ$

The relation between pressure drop of bed and standpipe was ob-

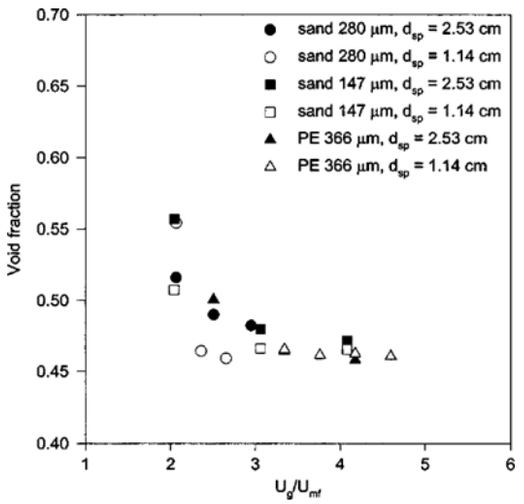

Fig. 8. The void fraction in the overflow standpipe for different gas velocity.

tained from the following equation [Geldart, 1986].

$$\Delta P_{sp}=\left(\frac{\Delta P_f}{L}\right)H_{sp} \tag{7}$$

The solid fraction in the overflow standpipe was determined by Eq. (6) and the effect of operating variables on the solid fraction is shown in Fig. 8.

Since the flow pattern is the fluidizing state in the underflow standpipe, the normal stress in the solid can be neglected. In a fluidized flow, τ_w and f can be calculated from Eqs. (8) and (9) [Levenspiel et al., 1991].

$$\tau_w=\frac{f W^2}{2\rho_s(1-\varepsilon)} \tag{8}$$

$$f=\frac{0.05}{U_s} \tag{9}$$

Applying Eq. (8) and (9) into Eq. (1) and integrating Eq. (1) gives Eq. (10) for the solid fraction in the underflow standpipe.

$$\Delta P_{sp}+\frac{2f W^2}{\rho_s(1-\varepsilon)d_{sp}}z-\rho_s(1-\varepsilon)gz+\frac{W^2}{\rho_s(1-\varepsilon)}=0 \tag{10}$$

The calculated solid fractions in the underflow standpipe are determined from Eq. (10) as shown in Fig. 9 at different operating conditions. As shown in Fig. 8 and Fig. 9, the void fraction in the underflow and overflow standpipe was estimated to be in the range of 0.8-0.9 and 0.45-0.55, respectively. Knowlton, et al. [1978] estimated the void fraction in the underflow standpipe with a valve at the exit of a 3 inch diameter standpipe to maintain the flow of 260 μm sand particle in the range of 0.16-0.7 ft/s gas velocity as packed bed mode and found that the void fraction was in the range of 0.35-0.43 by using the Ergun equation as in Eq. (11). Since solid flow in the standpipe was packed bed mode, Knowlton's prediction can be compared with the experimental data of the overflow standpipe in this study. In this case, the difference of void fraction was about 0.1 and this difference may come from the uncertainty in applying the U_r value for Ergun equation. Leung [1977] also estimated the void fraction in the industrial standpipes of 20 and 32 inch diameter. The employed particle was 80 μm alumina catalyst and the solid flow was the packed bed mode. Leung found from the pressure balance equations that the void fractions were in the range of 0.41-0.48 and these determined void fractions were in good agreement with the experimental data of the overflow standpipe in this study.

$$\frac{\Delta P}{H_{sp}}=\frac{150\mu(1-\varepsilon)^2U_r}{(\Phi d_p)^2\varepsilon^2}+\frac{1.75\rho_g(1-\varepsilon)U_r^2}{(\Phi d_p)\varepsilon} \tag{11}$$

Since the void fraction was calculated, the solid velocity in the standpipe can be calculated from the continuity equation as shown in Eq. (12).

$$W=A(1-\varepsilon)\rho_s U_s \tag{12}$$

The theoretically calculated solid velocities in the overflow and underflow standpipe are shown in Fig. 10 and Fig. 11. As shown in Fig. 10, the solid velocity in the overflow standpipe was in the

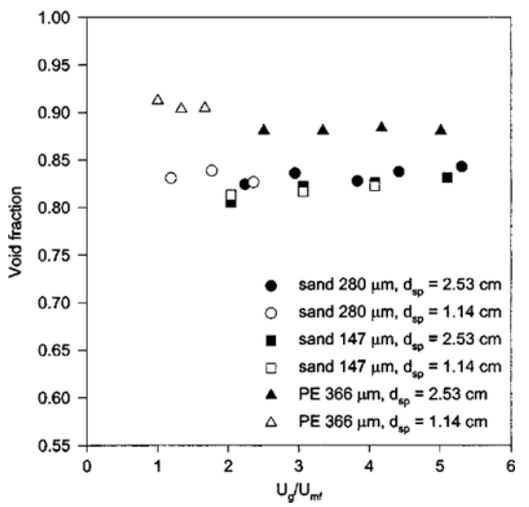

Fig. 9. The void fraction in the underflow standpipe for different gas velocity.

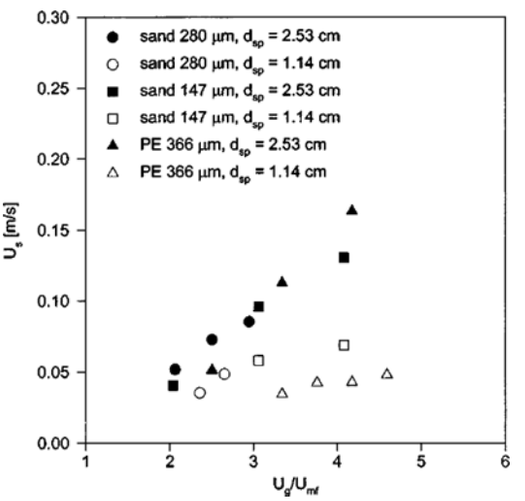

Fig. 10. Solid velocity in the overflow standpipe for different gas velocity.

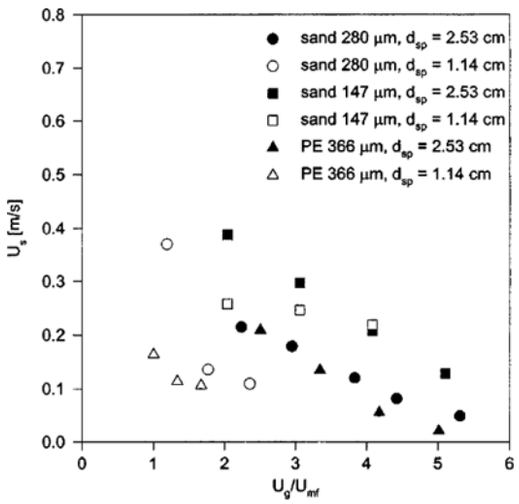

Fig. 11. Solid velocity in the underflow standpipe for different gas velocity.

range of 0.05-0.15 m/s, and solid velocity was increased with gas velocity. Rhodes [1998] obtained the solid velocity in the overflow standpipe of about 0.08 m/sec in the commercial fluidized bed system. Therefore, the prediction of void fraction and solid velocity in this study seems to be reasonable. Picciotti [1995] suggested that the solid velocity be kept as low as possible and recommended that the optimum value of solids velocity in the standpipe would be 0.15 m/s based on the considerations of erosion, solid surface characteristics, fines production and flux instability.

CONCLUSIONS

An experimental investigation of the characteristics of overflow and underflow standpipes was made with different standpipe configuration in the two fluidized bed system. From visual observation, it was found that the gas-solid suspension in the standpipe was packed bed flow for the overflow standpipe and dilute fluidized bed for the underflow standpipe.

In the overflow standpipe, solid mass flow rate increased with gas velocity at the lower velocity region and decreased with gas velocity at the higher gas velocity region. However, in the underflow standpipe, solid mass flow rate decreased with gas velocity and the effect of particle size on the solid mass flow rate was significant.

From the theoretical calculations based on the measured pressure drop, it was found that the void fraction in the underflow and overflow standpipe was found to be in the range of 0.8-0.9 and 0.45-0.55, respectively.

ACKNOWLEDGMENT

The authors would like to thank the R & D Management Center for Energy and Resources for its financial support.

NOMENCLATURE

A : area of standpipe [m^2]
d_p : average particle size [cm]
d_{sp} : diameter of standpipe [cm]
f : coefficient of friction between solid and wall surface [-]
G_g : gas flux [$kg/m^2 \cdot s$]
g : gravity acceleration [m/s^2]
H_{sp} : length of standpipe [cm]
L : length of fluidized reactor [cm]
$N_{Re,p}$: particle Reynolds number [-]
ΔP_t : total pressure drop in the fluidized bed [N/m^2]
ΔP_{sp} : pressure drop in the standpipe [N/m^2]
U_g : superficial gas velocity [m/s]
U_{mf} : superficial gas velocity at minimum fluidizing condition [m/s]
U_r : gas-solid relative velocity [m/s]
U_s : actual solid velocity [m/s]
W : solid flux [$kg/m^2 \cdot s$]
W_s : solid mass flow rate [kg/s]
z : axial coordinate in the standpipe [-]

Greek Letters

δ : internal angle of friction [degree]
ε : void fraction [-]
ε_{mf} : void fraction in a bed at minimum fluidizing condition [-]
ρ_s : density of particle [kg/m^3]
σ_z : average vertical normal stress in the solid [$kg/m \cdot s^2$]
σ_r : normal stress on pipe wall [$kg/m \cdot s^2$]
τ_w : shear stress [$kg/m \cdot s^2$]
μ_g :viscosity of gas [$kg/m \cdot s$]
Φ : sphericity of particle [-]

REFERENCES

Burkell, J. J., Grace, J. R., Zhao, J. and Lim, C. J., "Measurement of Solids Circulation Rates in Circulating Fluidized Beds," Circulating Fluidized Bed Technology II, Pergamon Press, 501 (1998).

Davidson, J. F., Clift, R. and Harrison, D., "Fluidization," 2nd ed., Academic Press (1985).

Geldart, D., "Gas Fluidization Technology," John Wiley & Sons (1986).

Ginestra, J. C., Rangachari, S. and Jackson, R., "A One-Dimensional Theory of Flow in a Vertical Standpipe," *Powder Technology*, **27**, 69 (1980).

Grace, J. R., Avidan, A. A. and Knowlton, T. M., "Circulating Fluidized Beds," Blackie Academic & Professional (1996).

Jones, P. J. and Leung, L. S., "Flow of Gas-Solid Mixtures in Standpipe. A Review," *Powder Technology*, **20**, 145 (1978).

Knowlton, T. M. and Hirsan, I., "L-valves Characterized for Solids Flow," *Hydrocarbon Processing*, **57**, 149 (1978).

Leung, L. S., "Design of Fluidized Gas-Solids Flow in Standpipes," *Powder Technology*, **16**, 1 (1977).

Leung, L. S., Jones, P. J. and Knowlton, T. M., "An Analysis of Moving-Bed Flow of Solids Down Standpipes and Slide Valves," *Powder Technology*, **19**, 7 (1978).

Leva, M., "Fluidization," McGraw-Hill, New York (1959).

Levenspil, O. and Kunii, D., "Fluidization Engineering," 2nd ed., Butterworth-Heinemann (1991).

Ozawa, M., Tobita, S., Mii, T. and Tomoyasu, Y., "Flow Pattern and Flow Behavior of Solid Particles in L-valve," Circulating Fluidized Bed Technology III, Pergamon Press, 615 (1991).
Picciotti, M., "Specify Standpipes and Feeder Valves for Packed Beds," Chemical Engineering Progress, January, 54 (1995).
Rhodes, M., "Introduction to Particle Technology," John Wiley & Sons (1998).
Rudolph, V., Chong, Y. O. and Nicklin, D. J., "Standpipe Modelling for Circulating Fluidized Beds," Circulating Fluidized Bed Technology III, Pergamon Press, 49 (1991).
Zhang, J.-Y. and Rudolph, V., "Flow Instability in Non-fluidized Standpipe Flow," *Powder Technology*, **97**, 109 (1998).